# Point Morphology - Additional Material

Stéphane Calderon  Tamy Boubekeur
Telecom Paristech - CNRS - IMT

## Abstract

This document completes the paper "Point Morphology", by Stéphane Calderon and Tamy Boubekeur (ACM Transaction on Graphics, Proc. of SIGGRAPH 2014). In part A, the appendix of the original paper is provided with extended elements of proof and discussion. In part B, additional results for the point morphology operators and example applications are provided.

## A Appendix

We derive a variational formulation of Mathematical Morphology and show that our projective approach is an approximation of this variational formulation.

In the following an input shape $I$ will be defined as a 3-manifold compact subset of $\mathbb{R}^3$. Moreover we will use this neighbourhood defintion: $\mathcal{N}^r_{\mathbf{x}} = \{\mathbf{u} \in \mathbb{R}^3, \|\mathbf{u}-\mathbf{x}\|_2 < r\}$.

First we recall the classical Mathematical Morphology which is based on set theory.

### A.1 Set Morphology

**Set Structuring Element.** *A Structuring Element $B$ is defined as follows:*

$$B \subset \mathbb{R}^3,\ \mathbf{0} \in B,\ B \text{ is compact and connected} \tag{1}$$

*And $B^\dagger$ is defined as the symmetric of $B$ w.r.t $\mathbf{0}$. The translated SE $B_{\mathbf{c}}$ with $\mathbf{c} \in \mathbb{R}^3$ is defined as:*

$$B_{\mathbf{c}} = \{\mathbf{b} + \mathbf{c} | \mathbf{b} \in B\} \tag{2}$$

**Set Morphology.** *Given an input shape $I$ and a SE $B$, the set Dilation is defined as:*

$$D_{I,B} = \bigcup_{\mathbf{c} \in I} B_{\mathbf{c}} \tag{3}$$

*The boundary associated with this set Dilation is defined from a topological point of view as:*

$$\partial D_{I,B} = \{\mathbf{x} \in \mathbb{R}^3,\ \forall r\ \exists\ (\hat{\mathbf{u}}, \check{\mathbf{u}}) \in \mathcal{N}^r_{\mathbf{x}} \mid \hat{\mathbf{u}} \in D_{I,B},\ \check{\mathbf{u}} \notin D_{I,B}\} \tag{4}$$

### A.2 Set Boundary Equivalence

**Equivalence Theorem.** *Given an input shape $I$ and a SE $B$ we have:*

$$D_{I,B} = \bigcup_{\mathbf{c} \in I} B_{\mathbf{c}} = \bigcup_{\mathbf{c} \in \partial I} B_{\mathbf{c}} \cup I \tag{5}$$

*Proof.* We have a second set characterization of $D_{I,B}$ (see [Serra 1983]) as:

$$D_{I,B} = \{\mathbf{x} \in \mathbb{R}^3 \mid B^\dagger_{\mathbf{x}} \cap I \neq \varnothing\} \tag{6}$$

Thus we have:

$$\bigcup_{\mathbf{c} \in \partial I} B_{\mathbf{c}} = \{\mathbf{x} \in \mathbb{R}^3 \mid B^\dagger_{\mathbf{x}} \cap \partial I \neq \varnothing\} \tag{7}$$

Let us first prove the first inclusion $\bigcup_{\mathbf{c} \in I} B_{\mathbf{c}} \subset \bigcup_{\mathbf{c} \in \partial I} B_{\mathbf{c}} \cup I$:

$$\mathbf{x}^* \in \bigcup_{\mathbf{c} \in I} B_{\mathbf{c}} \Rightarrow \mathbf{x}^* \in \{\mathbf{x} \in \mathbb{R}^3 \mid B^\dagger_{\mathbf{x}} \cap I \neq \varnothing\}$$
$$\Rightarrow \exists \mathbf{u} \in B^\dagger_{\mathbf{x}^*},\ \mathbf{u} \in I$$

If $\mathbf{x}^* \in I$ then :

$$\mathbf{x}^* \in \bigcup_{\mathbf{c} \in \partial I} B_{\mathbf{c}} \cup I \tag{8}$$

If $\mathbf{x}^* \notin I$ then there exists a continuous path $\mathscr{P}_{\mathbf{u},\mathbf{x}^*}$ between $\mathbf{u} \in I$ and $\mathbf{x}^* \notin I$ such as $\mathscr{P}_{\mathbf{u},\mathbf{x}^*} \subset B^\dagger_{\mathbf{x}^*}$ (since $B$ and $B^\dagger$ are connected). As a consequence:

$$\exists \mathbf{u}^* \in B^\dagger_{\mathbf{x}^*},\ \mathbf{u}^* \in \partial I \Rightarrow \mathbf{x}^* \in \{\mathbf{x} \in \mathbb{R}^3 \mid B^\dagger_{\mathbf{x}} \cap \partial I \neq \emptyset\}$$
$$\Rightarrow \mathbf{x}^* \in \bigcup_{\mathbf{c} \in \partial I} B_{\mathbf{c}} \cup I$$

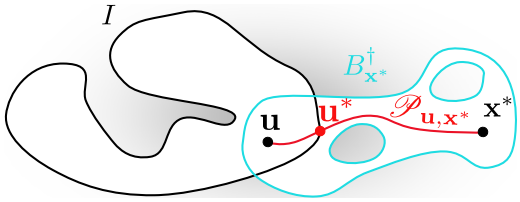


**Figure 1:** ***A2*** *Illustration of how $\mathscr{P}_{\mathbf{u},\mathbf{x}^*}$ crosses $I$'s boundary*

Let us prove the second inclusion $\bigcup_{\mathbf{c} \in \partial I} B_{\mathbf{c}} \cup I \subset \bigcup_{\mathbf{c} \in I} B_{\mathbf{c}}$:

$$\mathbf{x}^* \in \bigcup_{\mathbf{c} \in \partial I} B_{\mathbf{c}} \cup I$$

If $\mathbf{x}^* \in I$ then:

$$\mathbf{0} \in B \Rightarrow \mathbf{0} \in B^\dagger \Rightarrow \exists \mathbf{u} \in B^\dagger_{\mathbf{x}^*}, \mathbf{u} \in I$$
$$\Rightarrow \mathbf{x}^* \in \bigcup_{\mathbf{c} \in I} B_{\mathbf{c}}$$

If $\mathbf{x}^* \in \bigcup_{\mathbf{c} \in \partial I} B_{\mathbf{c}}$ owing the fact that $\partial I \subset I$ we have:

$$\mathbf{x}^* \in \bigcup_{\mathbf{c} \in I} B_{\mathbf{c}} \tag{9}$$

□

### A.3 Variational Morphology

We define a variational formulation of the set morphology.

**Variational Subset of $\mathbb{R}^3$.** *Given a compact subset $B$ of $\mathbb{R}^3$ we define its variational representation as a $\mathcal{C}^0$ scalar field $\mathscr{B} : \mathbb{R}^3 \to \mathbb{R}$ such as:*

$$\mathscr{B}(\mathbf{x}) = \begin{cases} < 0, & \text{if } \mathbf{x} \in \mathring{B} \\ 0, & \text{if } \mathbf{x} \in \partial B \\ > 0, & \text{if } \mathbf{x} \notin B \end{cases} \tag{10}$$

**Variational Structuring Element.** *Given a SE $B$ we define its variational SE representation as the variational representation $\mathscr{B}$ of $B$. We define a translated variational SE $\mathscr{B}_{\mathbf{c}}$ as:*

$$\mathscr{B}_{\mathbf{c}} : \mathbb{R}^3 \to \mathbb{R}, \mathbf{x} \to \mathscr{B}(\mathbf{x} - \mathbf{c}) \tag{11}$$

**Variational Morphology.** *Given an input shape $I$ and $B$ a SE with its variational SE representation $\mathscr{B}$ , we define a variational Dilation as:*

$$D_{I,\mathscr{B}}(\mathbf{x}) = \min_{\mathbf{c} \in I} \mathscr{B}_{\mathbf{c}}(\mathbf{x}) \tag{12}$$

*The boundary associated with this variational Dilation is defined as:*

$$\partial D_{I,\mathscr{B}} = \{\mathbf{x} \mid D_{I,\mathscr{B}}(\mathbf{x}) = 0\} \tag{13}$$

From this variational formulation we can derive $D_{I,\mathscr{B}}$ continuity.

**Lemma 1.** *Given an input shape $I$ and $B$ a SE with its variational SE representation $\mathscr{B}$, we have:*

$$D_{I,\mathscr{B}} : \mathbb{R}^3 \to \mathbb{R}, \mathbf{x} \to \min_{\mathbf{c} \in I} \mathscr{B}_{\mathbf{c}}(\mathbf{x}) \;\; is \;\; \mathcal{C}^0 \tag{14}$$

*Proof.* As $\mathscr{B}$ is $\mathcal{C}^0$ we get the continuity of $\mathscr{B}_{\mathbf{c}}(\mathbf{x}) = \mathscr{B}(\mathbf{x} - \mathbf{c})$ w.r.t $\mathbf{x}$ and $\mathbf{c}$ variables by composition. Adding that $I$ is a compact subset of $\mathbb{R}^3$ the lemma is a direct corollary of Berge's Maximum Theorem [Berge 1959]. □

**Lemma 2.** *Given an input shape $I$, and $B$ a SE with its variational SE $\mathscr{B}$ representation we have:*

$$\mathbf{x} \in D_{I,B} \Leftrightarrow D_{I,\mathscr{B}}(\mathbf{x}) \leqslant 0$$
$$\mathbf{x} \notin D_{I,B} \Leftrightarrow D_{I,\mathscr{B}}(\mathbf{x}) > 0$$

*Proof.* For the first equivalence we have:

$$\begin{aligned}
\mathbf{x} \in D_{I,B} &\Leftrightarrow \mathbf{x} \in \bigcup_{\mathbf{c} \in I} B_{\mathbf{c}} \\
&\Leftrightarrow \exists\, \hat{\mathbf{c}} \in I \mid \mathbf{x} \in B_{\hat{\mathbf{c}}} \\
&\Leftrightarrow \exists\, \hat{\mathbf{c}} \in I \mid \mathscr{B}_{\hat{\mathbf{c}}}(\mathbf{x}) \leqslant 0 \\
&\Leftrightarrow \min_{\mathbf{c} \in I} \mathscr{B}_{\mathbf{c}}(\mathbf{x}) \leqslant 0
\end{aligned}$$

and the second equivalence:

$$\begin{aligned}
\mathbf{x} \notin D_{I,B} &\Leftrightarrow \mathbf{x} \notin \bigcup_{\mathbf{c} \in I} B_{\mathbf{c}} \\
&\Leftrightarrow \forall\, \check{\mathbf{c}} \in I \; \mathbf{x} \notin B_{\check{\mathbf{c}}} \\
&\Leftrightarrow \forall\, \check{\mathbf{c}} \in I \; \mathscr{B}_{\check{\mathbf{c}}}(\mathbf{x}) > 0 \\
&\Leftrightarrow \min_{\mathbf{c} \in I} \mathscr{B}_{\mathbf{c}}(\mathbf{x}) > 0
\end{aligned}$$

□

### A.4 Set and Variational Formulation Equivalence

Now, we link set and variational morphologies in the form of an equality between the boundaries produced by both formulations.

**Equivalence Theorem.** *Given an input shape $I$ and $B$ a SE with its variational SE representation $\mathscr{B}$ we have:*

$$\partial D_{I,B} = \partial D_{I,\mathscr{B}} \tag{15}$$

*Proof.* Starting with the topological boundary definition $\partial D_{I,B}$ of $D_{I,B}$:

$$\mathbf{x} \in \partial D_{I,B} \Leftrightarrow \forall r\, \exists\, \hat{\mathbf{u}},\; \check{\mathbf{u}} \in \mathcal{N}_{\mathbf{x}}^{r} \mid \hat{\mathbf{u}} \in D_{I,B},\; \check{\mathbf{u}} \notin D_{I,B}$$
$$\mathbf{x} \in \partial D_{I,B} \Leftrightarrow \exists\, \hat{\mathbf{u}}_n,\; \check{\mathbf{u}}_n \underset{n \to \infty}{\to} \mathbf{x} \mid \hat{\mathbf{u}}_n \in D_{I,B},\; \check{\mathbf{u}}_n \notin D_{I,B}$$

With **Lemma 2** we have:

$$\mathbf{x} \in \partial D_{I,B} \Leftrightarrow \exists\, \hat{\mathbf{u}}_n,\; \check{\mathbf{u}}_n \underset{n \to \infty}{\to} \mathbf{x} \mid D_{I,\mathscr{B}}(\hat{\mathbf{u}}_n) \leqslant 0,\; D_{I,\mathscr{B}}(\check{\mathbf{u}}_n) > 0$$

By continuity of $\mathscr{D}_{I,B}$ (see **Lemma 1**) we have:

$$\mathbf{x} \in \partial D_{I,B} \Leftrightarrow D_{I,\mathscr{B}}(\mathbf{x}) = 0$$

And finally:

$$\mathbf{x} \in \partial D_{I,B} \Leftrightarrow \mathbf{x} \in \partial D_{I,\mathscr{B}}$$

□

### A.5 Variational Boundary Morphology

**Variational Boundary Morphology.** *Given an input shape $I$ with its variational representation $\mathscr{I}$ and $B$ a SE with its variational representation $\mathscr{B}$ , we define (with $\wedge$ as the binary $min$) a variational boundary Dilation as:*

$$D_{\mathscr{I},\mathscr{B}}(\mathbf{x}) = \min_{\substack{\mathbf{c} \in \mathbb{R}^3 \\ \mathscr{I}(\mathbf{c}) = 0}} \mathscr{B}_{\mathbf{c}}(\mathbf{x}) \;\wedge\; \mathscr{I}(\mathbf{x}) \tag{16}$$

*The boundary associated with this variational boundary Dilation is defined as:*

$$\partial D_{\mathscr{I},\mathscr{B}} = \{\mathbf{x} \mid D_{\mathscr{I},\mathscr{B}}(\mathbf{x}) = 0\} \tag{17}$$

### A.6 Set and Variational Boundary Formulation Equivalence

Now, we can show, similarly to variational morphology, but using the set boundary formulation as a basis, the same equivalence:

**Equivalence Theorem.** *Given an input shape $I$ with its variational representation $\mathscr{I}$ and $B$ a SE with its variational representation $\mathscr{B}$ we have:*

$$\partial D_{I,B} = \partial D_{\mathscr{I},\mathscr{B}} \tag{18}$$

### A.7 Projective Morphology

Given an input shape $I$ with its variational representation $\mathscr{I}$ and $B$ a SE with its variational representation $\mathscr{B}$ we define a projection operator to reach $\partial D_{\mathscr{I},\mathscr{B}}$

We start with this simple definition:

$$\mathcal{P}_{\mathscr{B}}(\mathbf{x}) = \mathbf{x} - \mathscr{B}_{\mathbf{c}*}(\mathbf{x}) \frac{\nabla \mathscr{B}_{\mathbf{c}*}(\mathbf{x})}{\|\nabla \mathscr{B}_{\mathbf{c}*}(\mathbf{x})\|} \tag{19}$$

$$\mathbf{c}^* = \underset{\substack{\mathbf{c} \in \mathbb{R}^3 \\ \mathscr{I}(\mathbf{c}) = 0}}{\operatorname{argmin}} \mathscr{B}_{\mathbf{c}}(\mathbf{x}) \tag{20}$$

We can show that using the same definitions from Sec. 3.4 for $\mathcal{P}_D^{\infty}$, but using an optimized centroid $\mathbf{c}^*$ defined as the exact solution of Eq. 20, we can reach the actual Dilation $\partial D_{\mathscr{I},\mathscr{B}}$:

**Projection Theorem.** *For $\mathbf{x} \in \mathbb{R}^3$:*

$$\mathcal{P}_D^{\infty}(\mathbf{x}) \in \partial D_{\mathscr{I},\mathscr{B}} \tag{21}$$

*Proof.* If the projection procedure converges toward $\mathcal{P}_D^\infty(\mathbf{x}) = \mathbf{x}^*$ we have $\mathcal{P}_D(\mathbf{x}^*) = \mathbf{x}^*$. This implies: :

$$\begin{cases} \mathscr{I}(\mathbf{x}^*) & > 0 \\ \mathcal{P}_{\mathscr{B}}(\mathbf{x}^*) & = \mathbf{x}^* \\ \mathscr{I}(\mathbf{c}^*) & = 0 \end{cases} \Leftrightarrow \begin{cases} \mathscr{I}(\mathbf{x}^*) & > 0 \\ \mathscr{B}_{\mathbf{c}*}(\mathbf{x}^*) & = 0 \\ \mathscr{I}(\mathbf{c}^*) & = 0 \end{cases} \tag{22}$$

Which permits to conclude:

$$\min_{\substack{\mathbf{c} \in \mathbb{R}^3 \\ \mathscr{I}(\mathbf{c})=0}} \mathscr{B}_{\mathbf{c}}(\mathbf{x}^*) = 0,\ \mathscr{I}(\mathbf{x}^*) > 0$$

$$\min_{\substack{\mathbf{c} \in \mathbb{R}^3 \\ \mathscr{I}(\mathbf{c})=0}} \mathscr{B}_{\mathbf{c}}(\mathbf{x}^*) \ \wedge\ \mathscr{I}(\mathbf{x}^*) = 0$$

$$D_{\mathscr{I},\mathscr{B}}(\mathbf{x}^*) = 0$$

$$\mathbf{x}^* \in \partial D_{\mathscr{I},\mathscr{B}}$$

□

The same hold for the Erosion operator $\mathcal{P}_E$.

### A.8 Point Morphology as a Sampled Projective Morphology

We can think of our morphological centroid as a sampled approximation of the projective morphology. We aim at reformulating Eq. 20 by a kernel density estimation of this global optimization problem with non linear constraints. We tackle this global optimization using the *mean shift* algorithm [Cheng 1995] on a sampling of its objective function. Thus, we replace Eq. 20 by:

$$\mathbf{c}^* = \underset{\substack{\mathbf{c} \in \mathbb{R}^3 \\ \mathscr{I}(\mathbf{p}_i)=0}}{\operatorname{argmin}} \sum_i (\mathscr{B}_{\mathbf{p}_i}(\mathbf{x}) + \gamma)\omega_\sigma\left(\|\mathbf{c} - \mathbf{p}_i\|_2\right) \tag{23}$$

This equation is a simple reformulation of Eq. 20 where the objective function $\mathscr{B}_{\mathbf{c}}(\mathbf{x})$ and the constraint $\mathscr{I}(\mathbf{c}) = 0$ are replaced by a new objective function based on weighted kernel density estimation. The constraint is replaced by kernel density samples, and the objective function by weights on theses samples. The global offset $\gamma = \min_{\mathbf{x} \in \mathbb{R}^3} \mathscr{B}(\mathbf{x})$ ensures the positiveness of the weights, and as such makes the objective a proper density. We found that using Gaussian kernels also for the weights improves stability. Additionally this also transform the initial minimization equation into the following maximization problem:

$$\mathbf{c}^* = \underset{\substack{\mathbf{c} \in \mathbb{R}^3 \\ \mathscr{I}(\mathbf{p}_i)=0}}{\operatorname{argmax}} \sum_i \omega_\sigma\left(\mathscr{B}_{\mathbf{p}_i}(\mathbf{x}) + \gamma\right)\omega_\sigma\left(\|\mathbf{c} - \mathbf{p}_i\|_2\right) \tag{24}$$

As a final step we instantiate the surface model $\mathscr{I}$ by the implicit form of a PSS model The new objective function of Eq. 24 can be maximized through the *mean shift* procedure [Fukunaga and Hostetler 1975; Cheng 1995].

$$\mathbf{c}^k(\mathbf{x}) = \sum_i \omega_\sigma(\|\mathbf{c}^{k-1}(\mathbf{x}) - \mathbf{p}_i\|)\ \omega_\sigma(\mathscr{B}_{\mathbf{p}_i}(\mathbf{x}))\mathbf{p}_i \tag{25}$$

$$\forall \boldsymbol{\pi}_i \in \Pi,\quad \mathscr{I}(\mathbf{p}_i) = 0 \tag{26}$$

### A.9 Normals of Point Morphology

The normals of the morphological surfaces are computed by taking the gradient of their implicit forms:

$$\mathbf{n}(\mathbf{x}) = \nabla\mathscr{B}_{\mathbf{c}*(\mathbf{x})}(\mathbf{x}) = \nabla\mathscr{B}_{\mathbf{c}*}(\mathbf{x})\nabla\mathbf{c}^*(\mathbf{x}) \tag{27}$$

We compute $\nabla\mathbf{c}^*(\mathbf{x})$ recursively through Eq. 25:

$$\nabla\mathbf{c}^k = \sum_i \omega_i^{k-1}\mathbf{p}_i\nabla\theta_i^{k-1} - \mathbf{c}^k\sum_i \omega_i^{k-1}\nabla\theta_i^{k-1} \tag{28}$$

$$\omega_i^{k-1} = \omega_\sigma(\|\mathbf{c}^{k-1} - \mathbf{p}_i\|)\ \omega_\sigma(\mathscr{B}_{\mathbf{p}_i}) \tag{29}$$

$$\nabla\theta_i^{k-1} = -\frac{2}{\sigma^2}((\mathbf{c}^{k-1} - \mathbf{p}_i)^T\nabla\mathbf{c}^{k-1} + \mathscr{B}_{\mathbf{p}_i}\nabla\mathscr{B}_{\mathbf{p}_i}) \tag{30}$$

### A.10 Empirical Convergence

We finally show an empirical validation of our point sampled approximation. We computed a reference high density sampling (1.6M points) of both the input hand (with the APSS surface model) and its 0.1 spherical dilation (with our Point Morphology). Then, starting from a low density input hand we compute the RMS error between its dilation and the reference dilated solution.

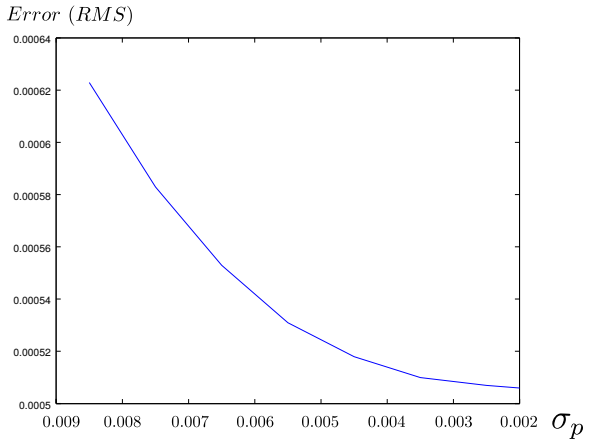


**Figure 2:** ***Convergence Rate.*** *We represent the RMS error between our Point Morphology and a reference solution. Here $\sigma_p$ represents the point spacing of the increasing density input models.*

## References


BERGE, C. 1959. *Espaces Topologiques, Fonctions multivoques*. Ed. Dunod, Paris.

CHENG, Y. 1995. Mean shift, mode seeking, and clustering. *IEEE Trans. Pattern Anal. Mach. Intell. 17*, 8 (Aug.), 790–799.

FUKUNAGA, K., AND HOSTETLER, L. D. 1975. The estimation of the gradient of a density function, with applications in pattern recognition. *IEEE Transactions on Information Theory 21*, 1, 32–40.

SERRA, J. 1983. *Image Analysis and Mathematical Morphology*. Academic Press, Inc., Orlando, FL, USA.


## B Additional Results

In the following pages, we provide additional examples of Point Morphology samplings and applications.

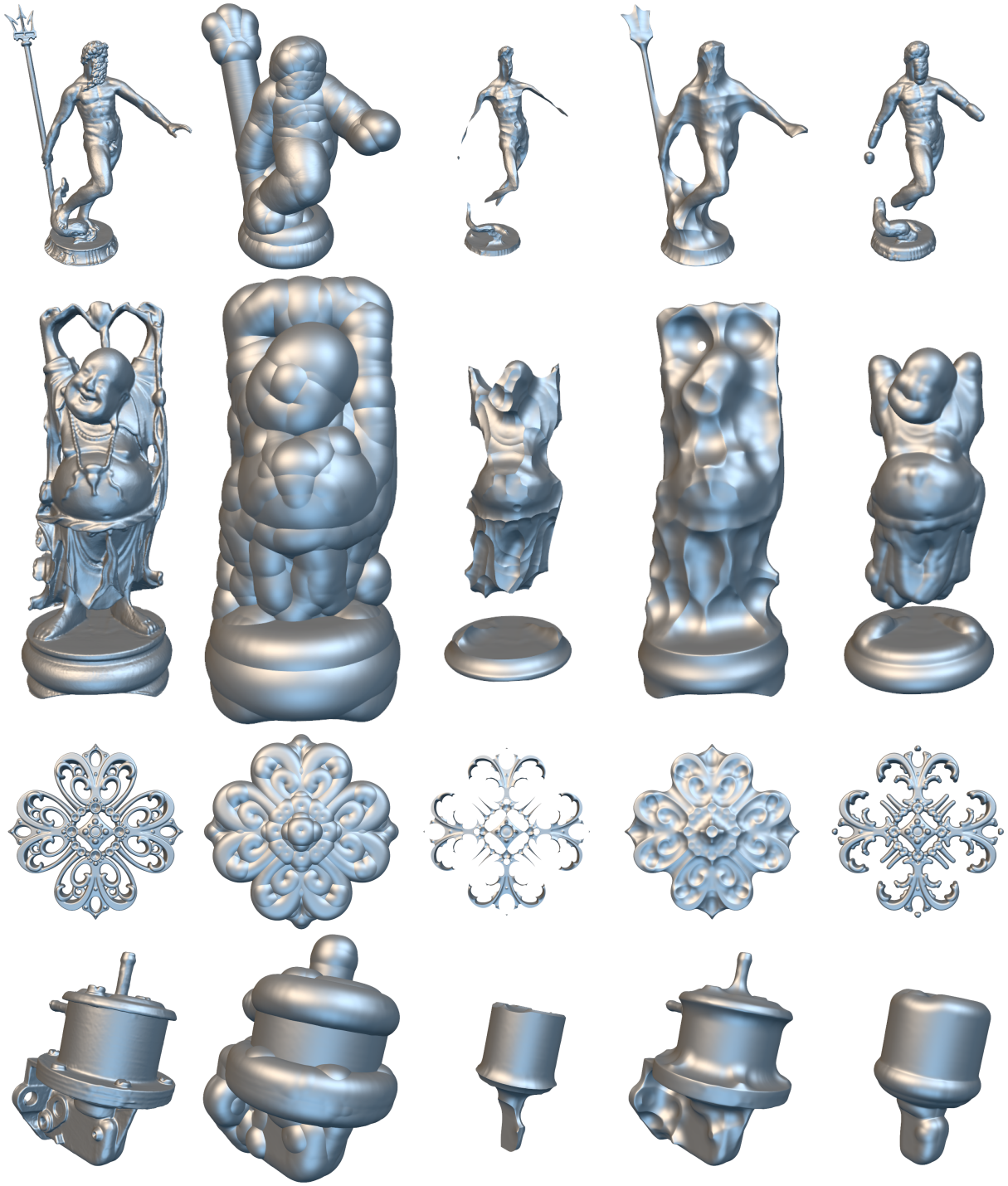

**Figure 3:** ***Point Morphology Operators.*** *From left to right: input, dilation, erosion, closing, opening for the Neptune (1st row, 1.2M input point), the Buddha (top, 255k input points), the Filigree (middle, 400k input points) and the Oil Pump (bottom, 390k input points).*

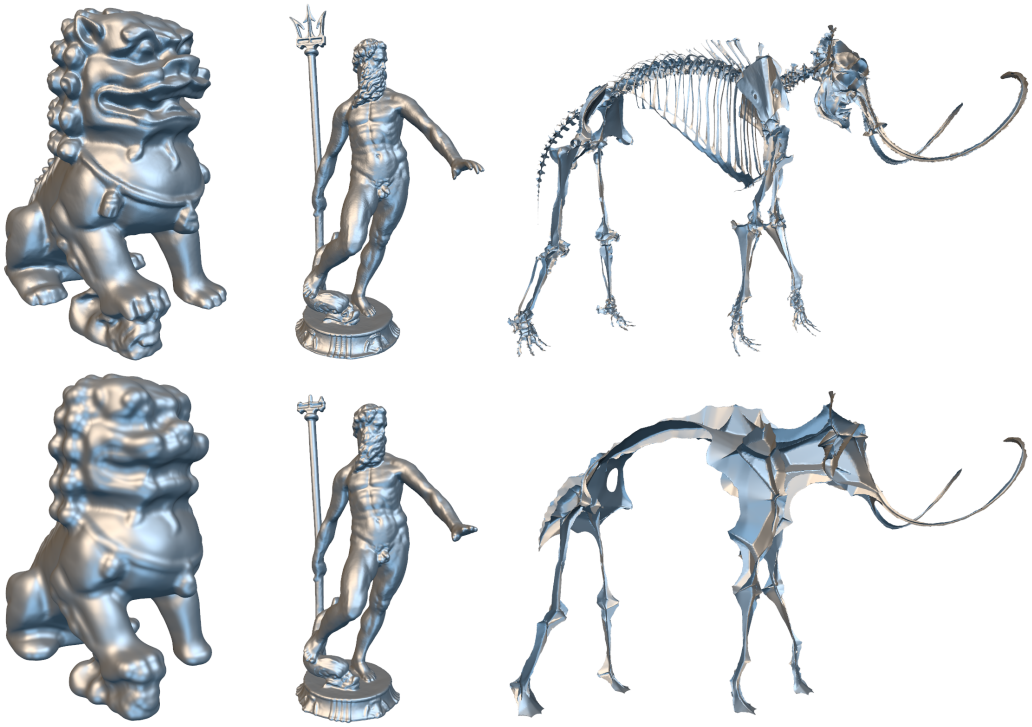

**Figure 4:** ***Hysteresis Shape Filtering*** *(bottom left and bottom middle) performed with Point Morphology on the Chinese Dragon (171k input points, with* $C_\Pi \circ 0_\Pi$ *and* $s_O = s_C = 0.05$*), the Neptune (1.2M input points,with* $O_\Pi \circ C_\Pi$ *and* $s_C = s_O = 0.008$*) and the Mammoth model (1.2M input points, with* $O_\Pi \circ C_\Pi$ *with* $s_C = 0.1$ *and* $s_O = 0.01$*) for which we display the resulting* ***filtered*** *projective medial axis (bottom right).*

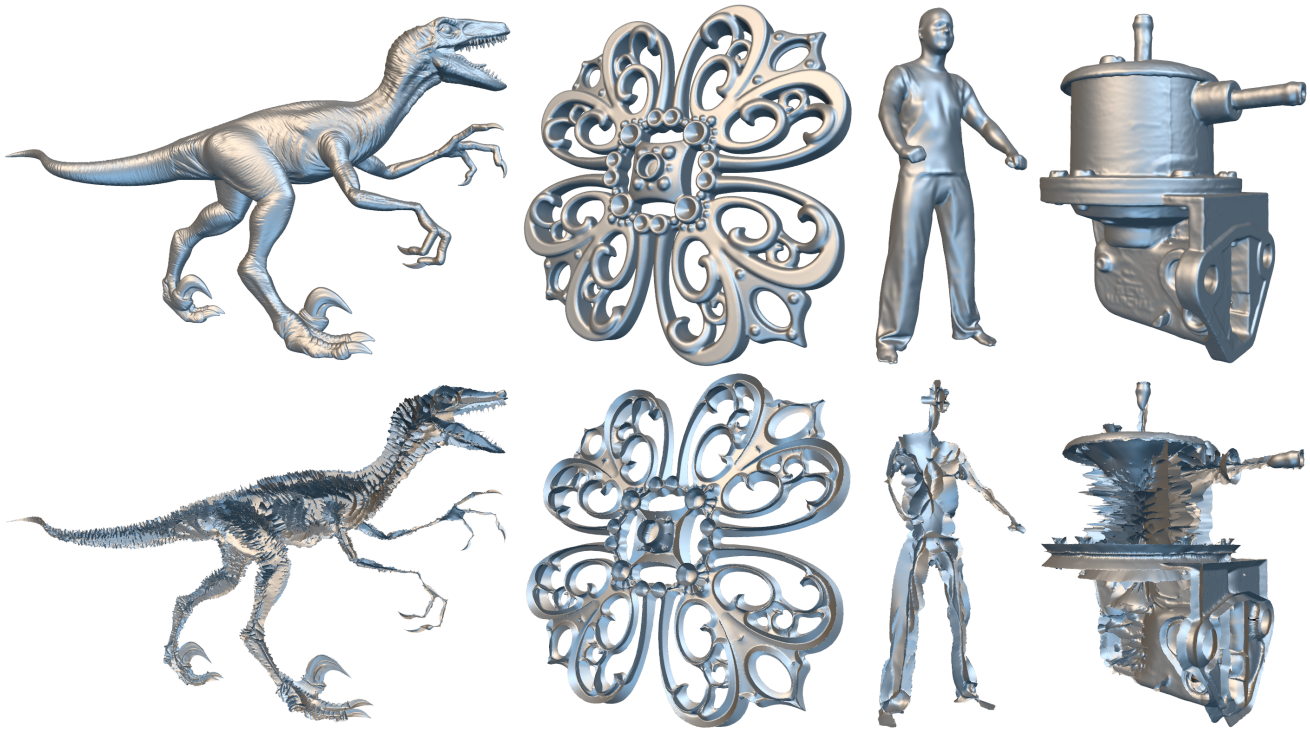

**Figure 5:** ***Projective Medial Axis*** *(bottom) computed with Point Morphology for the Raptor (880k input points), the Filigree (400k input points), a performance capture model (79k input points, courtesy Max Planck Institute, Germany) and the Oil Pump (390k input points).*

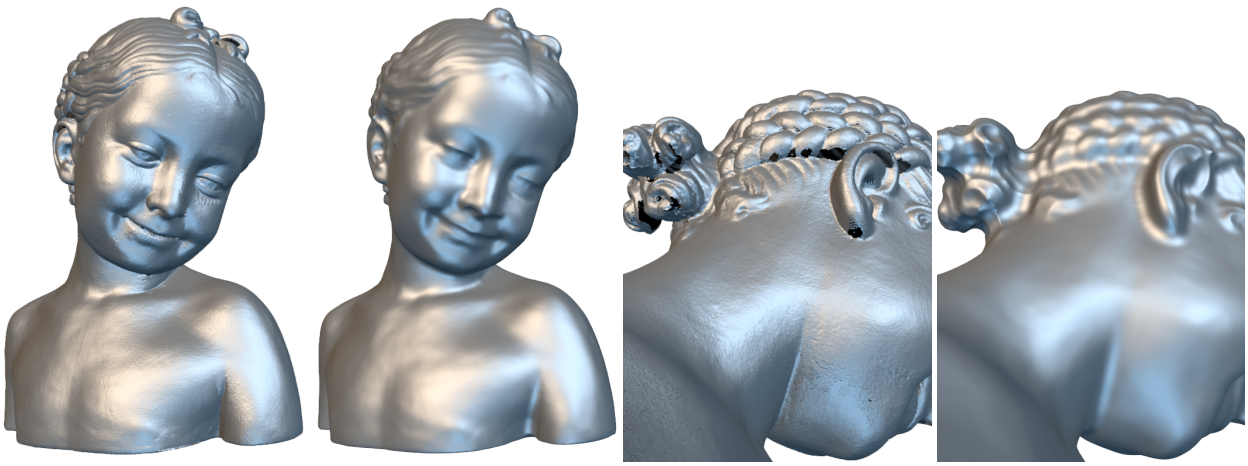

**Figure 6:** ***Raw ccan processing*** *for the Bimba model. From left to right: input raw scan (1.8M points), closing, input closeup, closing closeup*